

Study and Electrochemical Determination of Tyrosine at Graphene Nanosheets Composite Film Modified Glassy Carbon Electrode

M. Behpour*, S. Masoum, M. Meshki

Department of Analytical Chemistry, Faculty of chemistry, University of Kashan, Kashan, I. R. Iran

Article history:

Received 12/5/2013

Accepted 21/8/2013

Published online 1/9/2013

Keywords:

Graphene

Nanosheets

Modified glassy carbon electrode

Voltammetry

Tyrosine

Abstract

A graphene nanosheets (GNS) film coated glassy carbon electrode (GCE) was fabricated for sensitive determination of tyrosine (Tyr). The GNS-based sensor was characterized by scanning electron microscope and electrochemical impedance spectroscopy. The voltammetric techniques were employed to study electro-oxidation of Tyr. The results revealed that the modified electrode showed an electrocatalytic activity toward the anodic oxidation of Tyr by a marked enhancement in the current intensity and the shift in the oxidation potential to lower values (50 mV) in comparison with the bare GCE. Some kinetic parameters such as the electron transfer coefficient (α) were also determined for the Tyr oxidation. The detection limit for Tyr was found to be 2.0×10^{-8} M ($n=9$), and the peak current increases linearly with the Tyr concentration within the molar concentration ranges of 5.0×10^{-6} to 1.2×10^{-4} M. The modified electrode shows good sensitivity, selectivity and stability. The prepared electrode was applied for the determination of Tyr in real sample.

2013 JNS All rights reserved

**Corresponding author:*

E-mail address:

m.behpour@kashanu.ac.ir

Phone: 98 3615912352

Fax: +98 3615552375

1. Introduction

The electrochemical methods with chemically modified electrode (CMEs) have been widely used as sensitive and selective analytical methods for detection of the trace amounts of biologically important compounds [1-3]. In recent years, with the rapid development of nanostructure materials

and nanotechnology in the fields of biotechnology and medicine, considerable attention due to their novel properties have been received [4, 5].

It was P. R. Wallace in 1946 that first wrote on the band structure of graphene and showed the unusual semimetallic behaviour in this material. Since the discovery of graphene, more and more

attention is focused to develop the application of the properties of graphene and its derivatives, because unique properties, namely ballistic conductivity, high elasticity, very high mechanical strength, high surface area up to 2630 m²/g, and rapid heterogeneous electron transfer [6,7], make graphene as a good candidate in many technological aspects such as nanoelectronics, chemical/bio-sensors, nanocomposites, batteries, etc. Graphene is a two-dimensional sheet of sp² bonded carbon atoms, which can be viewed as an extra-large polycyclic aromatic molecule [8]. In addition, with the 2D structure, the monolayer graphene has its whole volume exposed to the environment, which can maximize the sensing effect. The principle of graphene devices is based on changes in device conductance due to chemical or biological species adsorbed on the surface of graphene, acting as electron donors or acceptors. Recently, graphene-based gas molecule sensors and biosensors have been reported [9-11].

Tyrosine, 4-hydroxyphenylalanine, is an essential aromatic amino acid precursor of important neurotransmitters such as dopamine. Tyrosine is indispensable for humans. It maintains a positive nitrogen balance [12,13] and its absence could produce albinism, hypochondria, or depression. In contrast, high tyrosine concentration in culture medium increases sister chromatid exchange. Tyrosine can be synthesized in the body from phenylalanine. It is hydrophobic and the phenolic hydroxyl of tyrosine is significantly more acidic. In addition, tyrosine has an antioxidant effect. Tyrosine is converted by skin cells into melanin, the dark pigment that protects against the harmful effects of ultraviolet light. It occurs in proteins that are part of signal transduction and also plays an important role in photosynthesis

[14,15]. Thus, tyrosine has been of great interest in research studies.

The development of analytical techniques for the rapid analysis of Tyr is important for quality and medical control. Numerous methods have been reported for tyrosine determination such as spectrophotometric, fluorimetric, flow injection, chemiluminescence, liquid chromatography–tandem mass spectrometry, gas chromatography–mass spectrometry and high-performance liquid chromatography [16-22]. A few studies involving electrochemical determination of Tyr have been reported [23,24].

The aim of this work is to fabricate a novel and stable electrochemical sensor for ultra sensitive determination of Tyr. In this paper, we described the preparation and application of a graphene nanosheets modified glassy carbon electrode (GNS/GCE) as a new sensor for the determination of Tyr in an aqueous buffer solution. Compared with bare electrode, the electro-reduction peak of Tyr was remarkably heightened at GNS modified electrode, and it can be used as an analytical sign for Tyr determination. In addition, we have examined the effect of various parameters on the electroactivity of modified electrode for electro-oxidation of Tyr. Also we have evaluated this method for the voltammetric determination of Tyr in real sample.

2. Experimental procedure

2.1. Instruments and chemicals

Voltammetric measurements were carried out by computerized potentiostat/ galvanostat μ Autolab (model PGSTAT30). The experiments were controlled with software, of general purpose electrochemical system (GPES) and NOVA. All the electrochemical studies were performed at 25±1 °C with a three electrode assembly, including

a 50 ml glass cell, an Ag/AgCl electrode as the reference electrode, and a platinum wire as the counter electrode. The working electrode was a modified glassy carbon electrode (2 mm diameter). The surface morphology of the modified electrode was observed using scanning electron microscopy (SEM) (Philips XL-30ESM). A metrohm pH meter model 691 was also used for pH measurements. Demineral water was produced with an ultra pure water system (smart 2 pure, TKA, Germany). All of the solutions were freshly prepared using demineral water.

The pure form of tyrosine (Tyr) was supplied by local pharmaceutical company (Iran). Graphene nanosheets (GNS) was obtained from the Chinese academy of sciences and had outside widths of 10.0– 20.0 nm, lengths of less than 1 - 2 μm and purities of over 95%. The phosphate buffer solutions were prepared from 0.1 M solutions of phosphoric acid in the pH range from 2.0 - 11.0

2.2 Preparation of GNS suspension and modified GCE

The GCE was carefully polished with 0.05 μm alumina slurry on a polishing cloth in sequence, and was then washed in an ultrasonic bath of methanol and water, respectively for 15 min. The GNSs were dispersed in DMF (4.0 mg GNSs per 1.0 ml) using ultrasonic agitation for 20 min, to obtain a homogeneous and stable suspension. The cleaned GCE was coated by casting 7.0 μl of the black suspension of GNSs and dried in the air.

3. Results and discussion

3.1. Electrochemical characterizations of the modified electrode

The *distribution of GNS/GCE* over the surface of modified glassy carbon electrode is shown by SEM image (Fig. 1).

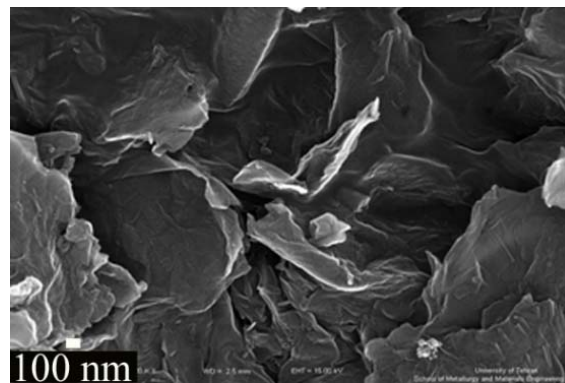


Fig. 1. SEM image of the GNS/GCE (scale bare is 100 nm).

Electrochemical impedance spectroscopy (EIS) was also employed to study the GNS/GCE. The Nyquist plot of the bare GCE and GNS/GCE in 0.1 M phosphate buffer solution (pH= 3.0) containing $5.0 \times 10^{-3}\text{M}$ $[\text{Fe}(\text{CN})_6]^{3-/4-}$ is shown in Fig. 2. It can be seen that the impedance spectrum of the bare GCE electrode exhibits two distinct regions: (1) a semicircle, related to the charge-transfer process; (2) a line defining a region of semi-infinite diffusion of species in the electrode. The value of the electron transfer resistance (R_{ct} , semicircle diameter) depends on the dielectric and insulating features at the electrode–electrolyte interface [25]. Significant difference of R_{ct} was observed upon the stepwise formation of the modified electrode. The R_{ct} values for the bare GCE and GNS/GCE were 1.22 $\text{k}\Omega$ and 0.1 $\text{k}\Omega$ respectively.

The experimental results for the Nyquist plots represented that GCE and GNS/GCE show the high and low charge transfer resistance, respectively. This might be due to the presence of the grapheme nanosheets film on the GCE that accelerates the transfer of the electrons at the surface of the electrode.

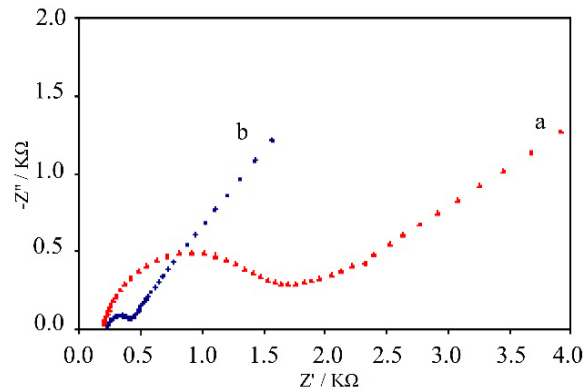


Fig. 2. The Nyquist plot of the bare GCE and GNS/GCE in 0.1 M phosphate buffer solution containing 5.0 mM $[\text{Fe}(\text{CN})_6]^{3-/4-}$.

After proving the presence of the modifier at the surface of the electrode by SEM and EIS, for an approximate estimate of the electrode-surface coverage of the electrode, cyclic voltammograms of this electrode obtained in the presence of probes solution of $\text{Fe}^{2+}/\text{Fe}^{3+}$ in 0.1 M phosphate buffer solution (pH= 3.0) at various scan rates (not show). The electrode-surface coverage was calculated by the method used by Sharp et al [26]. The peak current is related to the surface concentration of the electroactive species Γ by the following equation:

$$I_p = n^2 F^2 A \Gamma v / 4RT \quad (1)$$

Where n represents the number of electrons involved in the reaction; A is the surface area (0.0314 cm^2) of the GNS/GCE; Γ (mol cm^{-2}) is the surface coverage and the other symbols have their usual meanings. From the slope of the anodic peak current versus scan rate, the calculated surface concentration of GNS was $1.8 \times 10^{-6} \text{ mol cm}^{-2}$.

3.2. Electrochemical properties of Tyr at GNS/GCE

In order to test the potentiality of electrocatalytic activity of the GNS/GCE, its CV responses were obtained in phosphate buffer (pH= 3.0) at 50.0

mVs^{-1} . The obtained results demonstrate that the electro-oxidation of Tyr can be catalyzed by the addition of graphene nanosheets over the surface of GCE (Fig. 3). A remarkable increase in current and a decrease in potential were observed in the presence of $2.0 \times 10^{-5} \text{ M}$ Tyr. The obtained results showed that Tyr oxidation at bare GCE occurred with an anodic peak potential of 900.0 mV vs. Ag/AgCl (Fig. 3c), while its oxidation at GNS/GCE appeared at 850.0 mV vs. Ag/AgCl (Fig. 3d). Therefore, the oxidation of Tyr at the surface of GNS/GCE occurs at a potential about 50 mV toward less positive potential than of the bare GCE. On the other hand, the obtained data clearly shows that the addition of graphene nanosheets over the surface of GNS/GCE definitely improves the characteristics of Tyr oxidation.

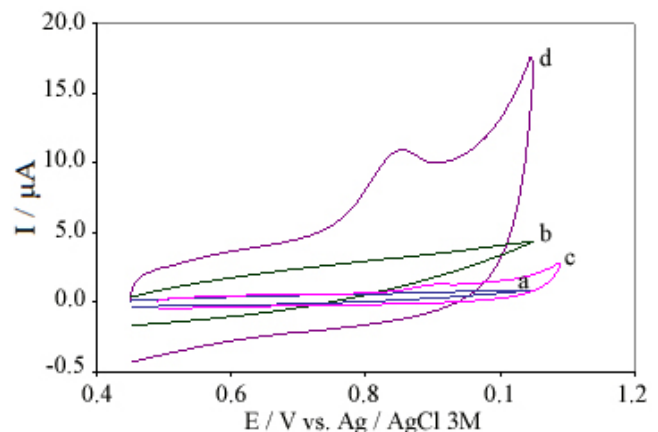


Fig. 3. Cyclic voltammograms of (a) bare GCE in buffer solution (pH= 3.0), (b) GNS/GCE in buffer solution (pH= 3.0), (c) bare GCE and (d) GNS/GCE in the presence of $2.0 \times 10^{-5} \text{ M}$ Tyr in phosphate buffer (pH= 3.0), scan rate: 50.0 mV/s.

3.3. Effects of pH

The effect of pH on the Tyr oxidation signal was investigated by cyclic voltammetry, using 0.1M phosphate solutions with pH values ranging from 2.0–11.0 and a scan rate of 20.0 mV s^{-1} (data not

shown). Within the pH range of 2.0 to 11.0, with 2.0×10^{-5} M Tyr in 0.1M phosphate buffer solutions, the oxidation potential of the electrochemical cell E_p shifted toward less positive potentials when the pH of Tyr solution increased, due to the hindrance of the oxidation at low concentrations of protons. The maximum anodic current of Tyr was obtained at pH = 3.0, using 0.1M phosphate buffer solutions. Thus pH of 3.0 was adopted for further studies. According to the Nernst equation (eq (2)), where n and m represents the number of electrons and protons involved in reaction, a and b represents the coefficients of the reagents in the reaction equation, a slope of 56.0 mV/pH, indicates that participation of the same protons and electrons in the electrochemical process. The dependence of E_p on the pH indicates that the electrochemical reaction involves proton transfer. The decrease of overpotential with increasing pH shows the catalytic effect of GNS/GCE on the oxidation of Tyr. Also, from the intercept of the curve of Fig. 4B, the standard formal potential (E°) of Tyr was obtained to be 1.34 V [24].

$$E = E^\circ + (0.0591/n) \log [(OX)^a/(R)^b] - (0.0591m/n) \text{pH} \quad (2)$$

$$E_{pa} \text{ (V vs. Ag/Ag Cl)} = 1.34 - 0.0545 \text{ pH}$$

3.4 Effect of scan rate

Useful information involving electrochemical mechanism can usually be acquired from the relationship between peak current and scan rate. Cyclic voltammograms of the GNS/GCE, in 0.1 M phosphate buffer solution containing 20.0 μM Tyr, with different scan rates is presented in Fig. 4. Inset A shows that the anodic oxidation currents of Tyr were proportional to the square root of the scan

rate indicating that at sufficiently positive potential the reaction is controlled by the diffusion of Tyr.

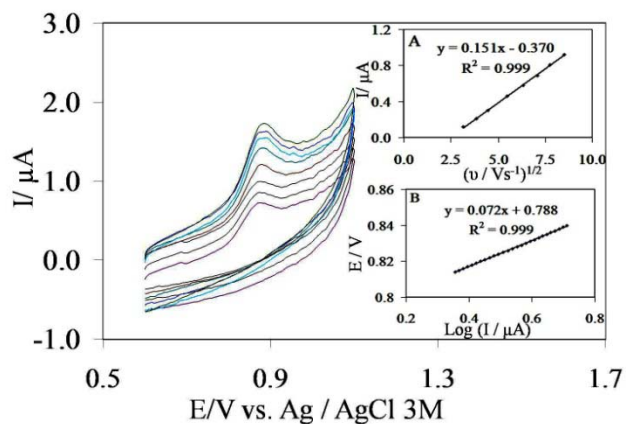


Fig. 4. Cyclic voltammograms of GNS/GCE in a phosphate buffer solution with pH = 3.0 for 2×10^{-5} M Tyr, using various scan rates: 10.0, 20.0, 30.0, 40.0, 50.0 and 90.0 mV s^{-1} (from inner to outer). (A) Plot of intensity: I vs. $V^{1/2}$. (B) Tafel plot, derived from the current potential curve, recorded at the scan rate of 20.0 mV s^{-1} .

A Tafel plot is a useful device for evaluating the kinetic parameters. Inset B of Fig. 4 shows the Tafel plot, drawn by using the data derived from the rising part of the current–voltage plot at a scan rate of 20.0 mV/s . According to Eq (3- 6): [27]

$$\eta = (2.3RT / n_a \alpha F) \log i^\circ + [2.3RT/n_a(1 - \alpha)F] \log i \quad (3)$$

$$\eta = a + b \log I \quad (4)$$

$$a = (2.3RT/n_a \alpha F) \log i^\circ \quad (5)$$

$$b = 2.3RT/n_a(1 - \alpha) F \quad (6)$$

The number of electrons involved in the rate-determining step (n_a) and the exchange current density (i°) can be estimated from the slope and the intercept, respectively, of the Tafel plot [26]. The obtained numerical value of 0.780 V decade⁻¹ for Tafel slope indicate a one-electron process for a rate-limiting step, assuming a charge transfer coefficient of $\alpha = 0.56$. Also, the value of i° was

found to be 0.40 mA cm^{-2} from the intercept of the Tafel plot.

3.5. Chronoamperometric measurements

The catalytic oxidation of Tyr by GNS/GCE was studied by chronoamperometry. Chronoamperograms obtained from solutions containing various concentrations of Tyr ranging - from 5.0 to 25.0 mM in phosphate buffer (pH=3.0) at GNS/GCE, using a potential step of 1000 mV (not shown). The diffusion coefficient (D) of Tyr in the modified electrode can be determined by chronoamperometric studies. For electroactive materials (Tyr in this case) with a diffusion coefficient of D the current for electrochemical reaction (at a mass transport limited rate) is described by the Cottrell equation: [27]

$$I = nFAD^{1/2}C_b \pi^{-1/2}t^{-1/2} \quad (7)$$

Where D and C_b are the diffusion coefficient ($\text{cm}^2 \text{ s}^{-1}$) and the bulk concentration (mol cm^{-3}), respectively. Under the diffusion control condition a plot of I vs. $t^{-1/2}$ will be linear, and from the slope, the value of D can be calculated. The mean value of the D was found to be $3.0 \times 10^{-5} \text{ cm}^2 \text{ s}^{-1}$.

3.6. Calibration curve and the detection limit

Since differential pulse voltammetry has several advantages compared to cyclic voltammetry, such as better resolution and negligible charging current contribution to the background current, it was applied to estimate the lower limit of detection of Tyr. Obtained Differential pulse voltammograms from the oxidation of various concentrations of Tyr at the GNS/GCE in 0.1 M phosphate buffer solution (pH=3.0) in the presence of different concentrations of Tyr are shown in Fig. 5. The inset in Fig. 5 shows the dependence of the oxidation peak current on the Tyr concentration that is linear for the different concentration range between 5.0 and 120.0 μM . The respective calibration equation for this concentration range

is:

$$i(\mu\text{A}) = 0.0371C(\mu\text{M}) + 0.0256 (R^2 = 0.9965) \quad (8)$$

From the analysis of this data, we estimate that the lower limit of detection of Tyr is of the order of $2.0 \times 10^{-8} \text{ M}$ (n=9). The relative standard deviation (R.S.D) was 1.23%, which showed excellent stability and reproducibility. Table 1 compares different modified electrodes that are used in the electrocatalysis of tyrosine.

Table 1. Comparison of different modified electrodes that are used in the electrocatalysis of Tyr.

Substrate	pH	Linear range/ μM	Detection limite/M	Ref
Nanostructures modified gold electrode	1.0	3.6-240.0	1.2×10^{-5}	14
(MWNTs)/4-aminobenzenesulfonic acid modified GCE	7.0	0.2-107.0	0.1×10^{-6}	28
Gold nanoparticle modified GCE	7.0	0.5-80.0	0.2×10^{-6}	29
Sodium dodecyl sulfate and gold nanoparticles modified CPE	3.0	0.1-10.0	5.5×10^{-8}	30
GNS/GCE	3.0	5.0-120.0	2.0×10^{-8}	Present study

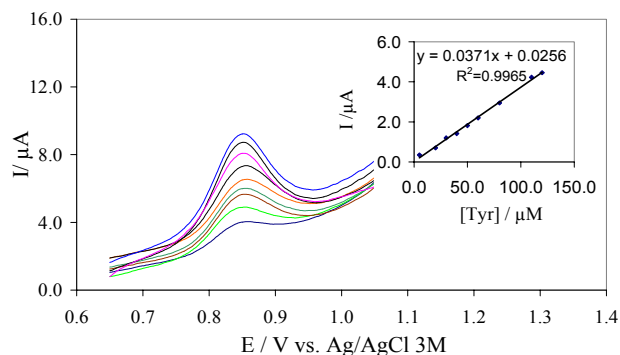


Fig. 5. Differential pulse voltammograms of GNS/GCE in 0.1 M phosphate buffer solution (pH= 3.0) containing 5.0, 20.0, 30.0, 40.0, 50.0, 60.0, 80.0, 110.0, 120.0 μM of Tyr. The inset shows the calibration curve.

3.7. The effect of the amount and injected volume of GNS composite

The optimum conditions for GNS composite film deposition was investigated by various amount and injected volume of GNS composite with voltammetry determination of Tyr. The results show that peak current reached a maximum at 7.0 μl of 4.0 mg of GNS composite and at higher values of GNS composite, a decrease in the signal was observed. This decrease in the signal was probably due to the aggregation of graphene nanosheets, which reduce the electroactive surface area.

3.8 Stability of GNS/GCE

The ability to generate a modified electrode with a reproducible surface was examined using DPV data obtained in optimized experimental conditions, from five prepared GNS/GCE separately. The RSD calculated for various parameters can be accepted as the criterion for a satisfactory surface reproducibility (1–5 %). This

degree of reproducibility is virtually the same as that expected for the renewal or ordinary glassy carbon electrode. Furthermore, the stability of the method was checked by successive DPV determination of a solution containing 50.0 mM Tyr for a two week period. When DPVs were recorded after the modified electrode, that was stored in an atmosphere at room temperature, the peak potentials for Tyr oxidation were decreased by less than 1.22 % and the current signals showed only less than 7.09 % decrease of the initial response. DPVs were recorded in the presence of Tyr at a scan rate of 100.0 mV s^{-1} . Therefore, at the surface of GNC/GCE, not only the sensitivity of Tyr increases, but also the fouling effects of the electrode and oxidation of Thy decrease.

3.9 Interference study

The influence of common interfering species was investigated in the presence of 20.0 μM Tyr. The tolerance limit was determined as the maximum concentration of the materials that caused a $\pm 5\%$ relative error in the determination of Tyr. The tolerated concentrations were 3.5×10^{-3} M for $\text{Ca}(\text{NO}_3)_2 \cdot 2 \text{H}_2\text{O}$, 2.1×10^{-3} M for NaNO_3 , 1.5×10^{-2} M for NH_4Cl and 1.0×10^{-3} M for penicillin, amoxicillin, erythromycin, ascorbic acid and dopamine. Also phenilanalyin and L-cyctein showed interference in five and two times determination of Tyr, respectively.

3.10 Analysis of Tyr in human blood serum

Human serum was selected as real sample for analysis by the proposed method using the standard addition method. For preparing the serum, 10.0 ml of blood was separated after putting the sample in

an incubator at 37.0°C for 30.0 min and centrifuging it. All samples were diluted with phosphate buffer (pH= 3.0) and then appropriate amounts of these diluted samples were transferred to the electrochemical cell. For the determination of each species using DPV and the potentials were controlled between – 0.2 and 1.2 V at the scan rate 20.0 mV s⁻¹. The data are given in Table 2.

Table 2. Determination of Tyr in human blood serum (n=4).

No.	Added (μM)	Found (μM)	Recovery (%)	RSD (%)
1	0.0	-	-	-
2	8.0	7.4	90.5	2.5
3	15.0	15.2	102.0	3.1
4	30.0	28.5	95.0	3.6

4. Conclusion

The present study demonstrates the construction of a GNS/GCE and its application for the determination of Tyr. The results show that the oxidation peak current of Tyr increased obviously and the oxidation peak potential shifted more negatively on GNS/GCE, indicating the excellent catalytic ability of the modified electrode. The detection limit of Tyr, the electron transfer coefficient (α), and diffusion coefficient (D) were calculated from differential pulses voltammetry, cyclic voltammetry and chronoamperometric responses. In addition, high sensitivity and selectivity, reproducibility of the voltammetric responses, low detection limit, ease of preparation and surface regeneration, makes the proposed modified electrode very useful for accurate determination of Tyr. Finally the results obtained in the analysis of Tyr in serum samples demonstrated the applicability of the method for real sample analysis.

Acknowledgements

The authors are grateful to University of Kashan for supporting this work by Grant. NO. 256450-4.

References

- [1] M. Behpour, S.M. Ghoreishi, E. Honarmand, M. Salavati-Niasari, *Analyst*. 136 (2011) 1979-1986.
- [2] M. Behpour, S.M. Ghoreishi, E. Honarmand, *Bull. Korean Chem. Soc.* 3 (2010) 845-849.
- [3] M. Behpour, S.M. Ghoreishi, E. Honarmand, M. Salavati-Niasari, *J. Appl. Electrochem.* 38 (2008) 833-838.
- [4] S.H. Huang, M.H. Liao, D.H. Chen, *Prog. Biotechnol.* 19 (2003) 1095-10100.
- [5] E. Katz, L. Sheeney, A.F. Buckmann, I. Willner, *Angew Chem. Int. Ed.* 41 (2002) 1343-1346.
- [6] M. Pumera, *Chem. Soc. Rev.* 39 (2010) 4146-1457.
- [7] L. Tang, J. Wang, K.P. Loh. *J. Am. Chem. Soc.* 132 (2010) 10976-10977.
- [8] D. Li, M.B. Müller, S. Gilje, R.B. Kaner, G.G. Wallace, *J. Nat. Nanotechnol.* 3 (2008) 101-105.
- [9] Y. Ohno, K. Maehashi, Y. Yamashiro, K. Matsumoto, *J. Nano Letters.* 9 (2009) 3318-3322.
- [10] F. Schedin, A.K. Geim, S.V. Morozov, E.W. Hill, P. Blake, M.I. Katsnelson, K.S. Novoselov, *J. Nature Materials.* 6 (2007) 652-655.
- [11] N. Mohanty, V. Berry, *J. Nano Letters.* (8) 2008 4469-4476.
- [12] B. Fang, H. Liu, G. Wang, Y. Zhou, M. Li, Y. Yu, *Ann. Chim.* 97 (2007) 1005-1013.
- [13] G.P. Jin, X.Q. Lin, *Electrochem. Commun.* 6(5) (2004) 454-460.

- [14] C. Quintana, S. Suarez, L. Hernandez, *Sensors and Actuators B: chemical*. 149 (2010) 129-135.
- [15] S. Chitravathi, B.E. Kumara Swamy, G.P. Mamatha, B.N. Chandrashekar, *J. Molecular Liquids* 172 (2012) 130-135.
- [16] Y. Azuma, M. Maekawa, Y. Kuwabara, T. Nakajima, K. Taniguchi, T. Kanno, *Clinical Chemistry* 35 (1989) 1399-1403.
- [17] F. Wang, K.Z. Wu, Y. Qing, Y.X. Ci, *Analytical Letters*.25 (1992) 1469-1478.
- [18] J.W. Costin, P.S. Francis, S.W. Lewis, *Analytica Chimica Acta*. 480 (2003) 67-77.
- [19] Y. Huang, X.Y. Jiang, W. Wang, *Talanta*. 70 (2006) 1157-1163.
- [20] H. Orhan, N.P.E. Vermeulen, C. Tump, H. Zappey, J.H.N. Meerman, *J. Chromatogr. B*. 799 (2004) 245-254.
- [21] C.H. Deng, Y.H. Deng, B. Wang, X.H. Yang, *J. Chromatogr. B*. 780 (2002) 407-413.
- [22] S. Letellier, J.P. Garnier, J. Spy, *J. Chromatogr. B*. 696 (1997) 9-17.
- [23] X. Yu, Z. Mai, Y. Xiao, X. Zou, *Electroanalysis*. 20 (2008) 1246-1251.
- [24] X. Tang, Y. Liu, H. Hou, T. You, *Talanta* 80 (2010) 2182-2186.
- [25] X.L.Luo, J.J.Xu, Q.Zhang, G.J.Yang, H.Y.Chen, *Biosen. and Bioelectron.* 21 (2005) 190-196.
- [26] M. Sharp, M. Petersson, K. Edstrom, *J. Electroanal. Chem.* 95 (1979) 123-130.
- [27] A.J. Bard, L.R. Faulkner, Wiley New York, 2002.
- [28] X. Tang, Y. Liu, H. Hou. T. you, *Talanta*.15 (2010) 2182-2186.
- [29] K. Qin Deng, J. Zhou, X. Fang Li, *Colloids Surf. B101* (2013) 183-188.
- [30] S.M. Ghoreishi, M. Delshad, A.Khoobi, *Cent. Eur. J. Chem.* 10 (2012) 1824-1829.